

## Effects of Polymer Additives on the Crystallization of Hydrates: A Molecular-Level Modulation

Fang Tian,\* Stefania Baldursdottir, and Jukka Rantanen

*Department of Pharmaceutics and Analytical Chemistry, Faculty of Pharmaceutical Sciences, University of Copenhagen, Denmark*

Received August 21, 2008; Revised Manuscript Received December 2, 2008; Accepted December 4, 2008

**Abstract:** The purpose of this study is to elucidate the effects of polymer additives on the growth behavior and final internal structure of hydrate crystals. The polymers used were poly(ethylene) glycol (PEG), ethyl(hydroxyethyl) cellulose (EHEC) and hydroxypropyl methylcellulose (HPMC). Rheological characterization of the polymer solutions was carried out. Nitrofurantoin and carbamazepine were crystallized separately from a mixture of acetone and polymer/water solution through evaporative crystallization. The crystallization process and final crystals were characterized by light microscopy, XRPD and FT-IR spectroscopy. PEG showed a minor viscosity increase, but polymer network associations were found in the EHEC and HPMC solutions. With no additive, nitrofurantoin crystallized as a mixture of plate-like (monohydrate I) and needle-like (monohydrate II) crystals. All polymers affected the crystalline phase, and HPMC and EHEC also changed the crystal morphology from needle-like to dendrite-like. H-Bonding was found to exist between these polymers (O–H group) and nitrofurantoin monohydrate (C=O group), while this was not the case with carbamazepine hydrate. Additives were able to modify the crystal phase and morphology due to H-bonding and polymer network properties. We envisage that the improved understanding of additives' role provided by this study can be utilized when designing control strategies for the crystallization process.

**Keywords:** Polymer; additives; hydrate; crystallization; H-bonding; network

### Introduction

Crystallization of active pharmaceutical ingredient (API) is the first step in manufacturing of solid dosage forms. Optimizing crystal properties by utilizing crystallization process could greatly facilitate the further manufacture of API. Several approaches have been employed in this area, including development of process monitoring and control strategies and application of various crystallization modifiers. Being among the most effective crystallization modifiers, polymer additives have recently attracted considerable interest. The presence of a certain amount of polymer additive could lead to a change in the crystal morphology, surface

properties and/or composition of the crystallizing phase.<sup>1–6</sup> The modification effect of polymer additives on drug crystals

- (1) Rasenack, N.; Müller, B. W. Ibuprofen crystals with optimized properties. *Int. J. Pharm.* **2002**, *245*, 9–24.
- (2) Nokhodchi, A.; Bolourtchian, N.; Dinarvand, R. Dissolution and mechanical behaviors of recrystallized carbamazepine from alcohol solution in the presence of additives. *J. Cryst. Growth* **2005**, *274*, 573–584.
- (3) Femi-Oyewo, M. N.; Spring, M. S. Studies on paracetamol crystals produced by growth in aqueous solutions. *Int. J. Pharm.* **1994**, *112*, 17–28.
- (4) Raghavan, S. L.; Trividic, A.; Davis, A. F.; Hadgraft, J. Crystallization of hydrocortisone acetate: influence of polymers. *Int. J. Pharm.* **2001**, *212*, 213–221.
- (5) Sikiric, M. D.; Furedi-Milhofer, H. The influence of surface active molecules on the crystallization of biominerals in solution. *Adv. Colloid Interface Sci.* **2006**, *128–130*, 135–158.
- (6) Petrova, R. I.; Patel, R.; Swift, J. A. Habit Modification of Asparagine Monohydrate Crystals by Growth in Hydrogel Media. *Cryst. Growth Des.* **2006**, *6*, 2709–2715.

\* Corresponding author. Mailing address: Dept. of Pharmaceutics and Analytical Chemistry, The Faculty of Pharmaceutical Sciences, University of Copenhagen, Universitetsparken 2, 2100 Copenhagen, Denmark. Tel: +45 35 33 61 41. Fax: +45 35 33 60 30. E-mail: ft@farma.ku.dk.

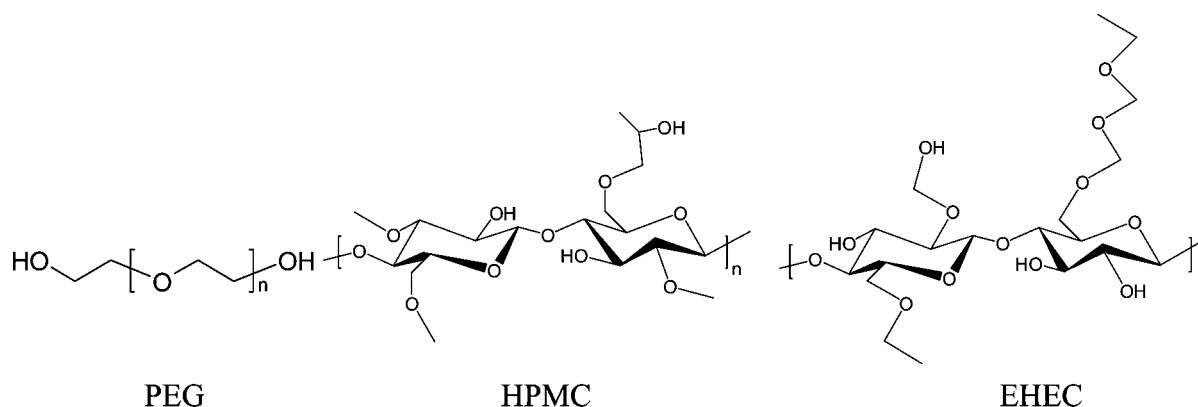


**Figure 1.** Chemical structures of polymers used in this study (the degree of subgroup substitution is not known).

is suggested to be selective adsorption of the additives at the crystal/solution interface, where the main driving force ranges from purely electrostatic to highly specific recognition of crystal phases by the polymer. Various experimental methods have been applied for investigation of the underlying mechanism, e.g. HPLC and solid state molecular spectroscopic techniques.<sup>7–10</sup> Due to the complex nature and relative weakness of additive–drug interactions in aqueous environments, as well as the detection limit of currently available techniques, our understanding of the kinetic process that occurs between additive and drug during crystallization so far is poor. This also limits the use of additives as an effective part of optimizing the crystallization process. Moreover, though polymers are commonly used in pharmaceutical formulations and have been widely used in the pharmaceutical crystallization investigations as listed above, studies on polymer behavior in these systems are extremely limited.

The model pharmaceutical compound chosen in this study is nitrofurantoin (NF). It is an antibiotic commonly used in the treatment of urinary tract infection and can exist as two anhydrate forms under dry conditions. The interesting feature of this drug is that it has flexible hydrogen bonding sites (as shown later in Figure 10). Also, nitrofurantoin molecules in the monohydrate structure can H-bond differently with water molecules and can thus arrange into two different crystalline forms in aqueous environments, which have been assigned as monohydrate I and II.<sup>11,12</sup> Until now, only three publications have reported on the observation of monohydrate I,<sup>11–13</sup> and it was found to be an impurity during the crystallization of NF monohydrate II.<sup>13</sup> No further discussions can be found on the crystallization of NF monohydrates. Carbamazepine, having only one hydrate form as compared to NF which has two reported monohydrate structures, was employed as model compound.<sup>14</sup>

In this study, crystallization was performed from three different polymer solutions. The rheological behavior of the polymers was evaluated in order to discover the possible relationship between these rheological properties and the final crystal properties, including morphology and crystalline form. A particular purpose of this study is also to explore the crystallization mechanism of two structurally different NF monohydrates, and to control its crystallization further through suitable additives.

## Materials and Methods

**Materials.** The polymers used in this study were poly(ethylene) glycol (PEG; Simon & Werner GmbH, Germany), molecular weight ( $M_w$ ) = 20 000, hydroxypropyl methylcellulose (HPMC; Metolose 90SH 4000 SR, Shin Etsu, Japan),  $M_w$  = 40 000, and ethyl(hydroxyethyl) cellulose (EHEC; BERMOCOLL E 230 X, Akzo Nobel Functional Chemicals AB, Stenungsund, Sweden),  $M_w$  = 150 000. The basic structures of the polymers are shown in Figure 1.

For the crystallization study, 0.075 g of drug powder (nitrofurantoin or carbamazepine, used as purchased) was dissolved separately in 30 cm<sup>3</sup> of acetone and polymer/water solution (1.0 wt %, volume ratio 2:1). The purchased NF (from Unikem A/S, Copenhagen, Denmark) and CBZ (Minneapolis, MN 55413) powder were identified as stable

- (7) Wikström, H.; Carroll, W. J.; Taylor, L. S. Manipulating Theophylline Monohydrate Formation During High-Shear Wet Granulation Through Improved Understanding of the Role of Pharmaceutical Excipients. *Pharm. Res.* **2008**, *25*, 923–935.
- (8) Zimmermann, A.; Ringkjøbing Elema, M.; Hansen, T.; Müllertz, A.; Hovgaard, L. Determination of surface-adsorbed excipients of various types on drug particles prepared by antisolvent precipitation using HPLC with evaporative light scattering detection. *J. Pharm. Biomed. Anal.* **2007**, *44*, 874–880.
- (9) Otsuka, M.; Ohfusa, T.; Matsuda, Y. Effect of binders on polymorphic transformation kinetics of carbamazepine in aqueous solution. *Colloids Surf., B* **2000**, *17*, 145–152.
- (10) Otsuka, M.; Ishii, M.; Matsuda, Y. Effect of surface-modification on hydration kinetics of nitrofurantoin anhydrate. *Colloids Surf., B* **2002**, *23*, 73–82.
- (11) Caira, M. R.; Pienaar, E. W.; Loetter, A. P. Polymorphism and pseudopolymorphism of the antibacterial nitrofurantoin. *Mol. Cryst. Liq. Cryst. Sci. Technol., A: Mol. Cryst. Liq. Cryst.* **1996**, *279*, 241–264.
- (12) Pienaar, E. W.; Caira, M. R.; Lotter, A. P. Polymorphs of nitrofurantoin. I. Preparation and x-ray crystal structures of two monohydrated forms of nitrofurantoin. *J. Crystallogr. Spectrosc. Res.* **1993**, *23*, 739–44.
- (13) Kelly, R. C. A molecular approach to understanding the directed nucleation and phase transformation of carbamazepine and nitrofurantoin in aqueous and organic solutions (Dissertation); The University of Michigan: Ann Arbor, MI, 2003.
- (14) Reboul, P. J.; Cristau, B.; Soyfer, J. C. 5H-Dibenz[b,f]azepine-5-carboxamide (carbamazepine). *Acta Crystallogr.* **1981**, *B37*, 1844–1848.

$\beta$ -polymorph (CSD refcode LABJON02<sup>12</sup>) and polymorph III (CSD refcode CBMZPN01<sup>14</sup>) respectively. The solution vessels were then left to allow slow solvent evaporation, and the resulting final crystals were characterized by several solid state techniques.

**Characterization methods. (a) Rheology Measurements.** Oscillatory shear and viscosity experiments were conducted in a TA AR-G2 rheometer using a cone-and-plate geometry with a cone angle of 1° and a diameter of 60 mm. A cover was placed over the cone to reduce evaporation of the acetone as much as possible during measurement. The measuring device is equipped with a temperature unit (Peltier plate) that gives very good temperature control over extended lengths of time. The experiments were conducted at 25 °C. The viscosity measurements were conducted over an extended shear rate range (covering both the linear and nonlinear viscoelastic regimes). The shear rate dependence of the viscosity was monitored as a function of increasing shear rate. This method can be used to detect shear thinning and/or shear thickening features in polymer systems. The shear thinning behavior occurs when intermolecular associations and/or entanglements are broken apart by shear forces. Extensive shear thinning at high shear rates is usually observed for strongly entangled or associated systems.<sup>15</sup>

In oscillatory shear measurements, the sample is placed under periodically varied stress, i.e., sinusoidal alteration at an angular frequency,  $\omega$ . This allows measurement of the storage modulus ( $G'$ ), the elastic response in the system, the loss modulus ( $G''$ ) and the viscous properties of the system. Most polymer systems are viscoelastic and therefore have a combination of elastic and viscous properties. The complex viscosity ( $\eta^*$ ) takes into account both the viscosity aspect and the elasticity aspect of the viscosity (eq 1).

$$\eta^*(\omega) = \frac{\sqrt{G'(\omega)^2 + G''(\omega)^2}}{\omega} \quad (1)$$

The complex viscosity ( $\eta^*$ ) shows an angular frequency dependency on the analogy of the observed shear dependency of the shear viscosity. This phenomenon can be further described with the power law exponent  $\nu$ , obtained from the relation  $\eta^* \sim \omega^{-\nu}$ . Strong frequency dependence is typical for systems with intermolecular associations and for entangled chain networks.<sup>16</sup> All the oscillatory shear experiments were performed within the linear viscoelastic regime, where the dynamic storage modulus ( $G'$ ) and loss modulus ( $G''$ ) are independent of the oscillation torque.

**(b) Light Microscopy.** The morphology of crystals produced during the crystallization process was observed using a Zeiss Axiolab microscope (Carl Zeiss, Inc., Beograd, Austria) and recorded every 20 s by a DeltaPix digital camera (Maalov, Denmark). DeltaPix software 1.6 (Maalov, Denmark) was used for data acquisition.

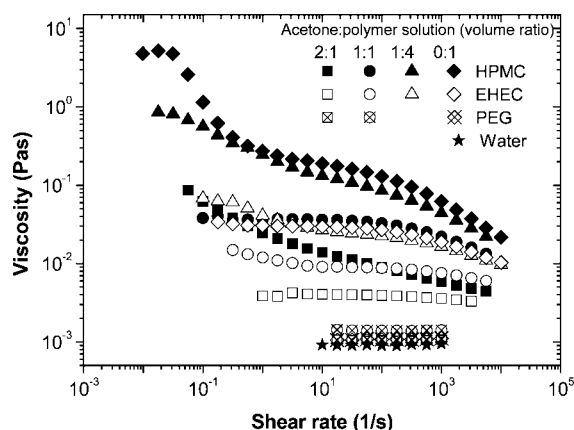


**Figure 2.** Viscosity as a function of shear rate for the three different polymer systems, PEG, EHEC and HPMC compared to pure water. The numbers shown above are in volume ratio, and the decreasing volume ratio of acetone represents the evaporation occurring in the system.

**(c) X-ray Powder Diffraction (XRPD).** X-ray powder diffractograms were measured on a PANalytical X'Pert PRO X-ray diffractometer (Almelo, Netherlands) using Cu K $\alpha_1$  radiation ( $\lambda = 1.5406$  Å). The voltage and current were 45 kV and 40 mA respectively. Samples were measured in reflection mode in the  $2\theta$ -range 5–40° using an X'celerator detector; the resolution was 0.0334 °2 $\theta$ . Data were collected using X'Pert Data Collector and viewed using X'Pert Data Viewer (PANalytical B.V., The Netherlands).

**(d) FT-IR Spectroscopy.** Each sample was physically mixed with KBr at a concentration of 0.5 wt %. The powder mixtures (250 mg) were gently ground and then compressed into a pellet of 12 mm  $\phi$ . The spectra of all the samples were measured at the absorption mode using a BOMEN MB155 spectrophotometer with 64 scans and a resolution of 4 cm<sup>-1</sup>.

**(e) Crystal Structure Visualization.** Crystal structures of nitrofurantoin monohydrate I, II and carbamazepine dihydrate were obtained from Cambridge Structural Database (CSD refcode HAXBUD01,<sup>12</sup> HAXBUD<sup>12</sup> and FEFNOT02<sup>17</sup> respectively) and visualized using the software Mercury 1.4.2 (Cambridge Crystallographic Data Centre, U.K.).

## Results

**Rheological Properties of the Polymer Solutions.** Figure 2 shows the effect of shear rate on the measured viscosity for the different polymer systems, PEG, EHEC and HPMC (1 wt %). The decreasing amount of acetone was used to describe the solvent condition during evaporation and thus also the rheological properties of polymers during the

(15) Sperling, L. H. Polymer network definitions. *Polym. Mater. Sci. Eng.* **1998**, 79, 536.

(16) Winter, H. H.; Chambon, F. Analysis of linear viscoelasticity of a crosslinking polymer at the gel point. *J. Rheol.* **1986**, 30 (2), 367–382.

(17) Harris, R. K.; Ghi, P. Y.; Puschmann, H.; Apperley, D. C.; Griesser, U. J.; Hammond, R. B.; Ma, C.; Roberts, K. J.; Pearce, G. J.; Yates, J. R.; Pickard, C. J. Structural Studies of the Polymorphs of Carbamazepine, Its Dihydrate, and Two Solvates. *Org. Process Res. Dev.* **2005**, 9, 902–910.

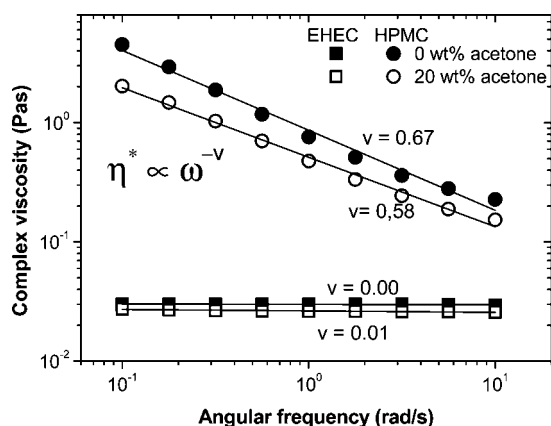


**Figure 3.** Frequency dependency of the complex viscosity of the two polymer systems, with acetone:polymer solution ratios of 0:1 (no acetone) or 1:4 (20 wt % acetone).

crystallization process. The shear rate dependence on the viscosity was detected for all the HPMC systems and the EHEC solutions, except for the most diluted one. The shear thinning observed can be ascribed to the disruption of entanglements and other intermolecular interactions. The PEG solutions only had a minor influence on the viscosity of the solution when compared with pure water, but did not show any signs of shear dependency, indicating a Newtonian fluid with very low viscosity.

Figure 3 shows the frequency dependency of the complex viscosity of the EHEC and HPMC systems with acetone:polymer solution ratios of 0:1 (no acetone) and 1:4 (20 wt % acetone). The frequency dependence of the complex viscosity can be quantified by  $\eta^* \sim \omega^{-\nu}$  ( $0 \leq \nu \leq 1$ ). Low values of  $\nu$  indicate viscous-like behavior, while higher values indicate a more elastic response.<sup>18</sup> Both the EHEC systems had a  $\nu$  value of 0.0, the viscous mode being dominant in the system, independently of the amount of acetone. The values of  $\nu$  were higher for the HPMC systems, indicating more solid-like behavior. This illustrates that there were relatively few cross-links in the EHEC system, while for the HPMC system it showed more associations and more elastic response. The values of  $\nu$  also increased with decreasing amounts of acetone in the HPMC system, indicating the growing associations in the system with evaporation.

**The Effect of Additive on the Crystallization of Nitrofurantion and Carbamazepine. (a) Microscopic Observation.** Crystallization of NF from acetone–water mixture with no additive resulted in a mixed needle cluster and plate-like crystals as observed under light microscopy (Figure 4a). This, however, appeared to change in the presence of excipients. In the solution containing PEG, the final crystals were crystallized as needle clusters without any noticeable plate-like crystals (Figure 4b). Neither the plate-like crystals nor the characteristic needle clusters could be

observed in the presence of EHEC or HPMC (Figure 4c,d). Instead, all the crystals were of dendrite-like morphology. A certain difference in density was also noticed in the branches, where more condensed branches were formed when NF was crystallized from the solution containing HPMC. In order to gain an understanding of the growth mechanism of dendrite-like crystals, their formation process was also followed visually (Figure 5).

CBZ was crystallized under the same conditions in the presence of each of the three polymer additives to allow comparison (Figure 6). None of the polymers demonstrated any obvious influence on the final crystal morphology. However, slight changes were observed for the CBZ crystals grown in the presence of EHEC and HPMC (Figures 6c and 6d), where the needles appeared to be greatly shortened, especially in the major growth direction, indicating a certain influence from these two polymers. This will be explained in further detail later.

**(b) XRPD.** To confirm the crystalline composition, the crystals shown above were measured by XRPD (Figure 7). The XRPD diffractograms of NF  $\beta$ -polymorph, monohydrate I and II powder samples were plotted together for a better comparison (Figure 7a–c).

The XRPD pattern of NF crystallized from solution in the absence of polymer (Figure 7d) demonstrated mixed reflections from both monohydrates I and II. When NF was crystallized in the presence of additives (Figure 7e–g), however, the XRPD diffractograms showed a pattern similar to that of pure NF monohydrate II (Figure 7c), and no reflections from monohydrate I could be detected. The characteristic reflections at 10.14, 14.06 and 21.52 ( $^{\circ}2\theta$ ) of monohydrate II from crystal planes (002), (200) and (104), respectively, could be observed in all these diffractograms, although there were some differences in relative intensity, especially for that crystallized from solution containing PEG.

XRPD diffractograms of all the CBZ samples were identical to that of pure CBZ dihydrate, which indicates that the presence of polymers had no influence on the crystallization outcome of CBZ.

**(c) FT-IR.** FT-IR spectra of NF stable  $\beta$ -polymorph and monohydrate I and II (Figures 8b and 8c respectively) compared well to that reported earlier.<sup>11</sup> The most distinguishing spectral differences between the two monohydrates were observed for O–H and C=O bands (as shaded in black and gray, respectively, in Figure 8). In the spectrum of monohydrate I, a small shoulder at around 1789  $\text{cm}^{-1}$  was caused by non-hydrogen bonded C=O bands, and a peak at around 1728  $\text{cm}^{-1}$  was associated with hydrogen bonded C=O (shaded in gray in Figure 8b). In monohydrate II, the peak position of the non-hydrogen bonded C=O, however, was slightly broader, while also the hydrogen bonded C=O exhibited only one sharp peak (Figure 8c).

The IR spectra of NF crystallized from solvents without any polymer (Figure 8d) seem to be more dominated by the spectrum of monohydrate II. This is in contrast to those

(18) Winter, H. H. Transient Networks. Evolution of rheology during chemical gelation. *Prog. Colloid Polym. Sci.* **1987**, 75, 104–110.

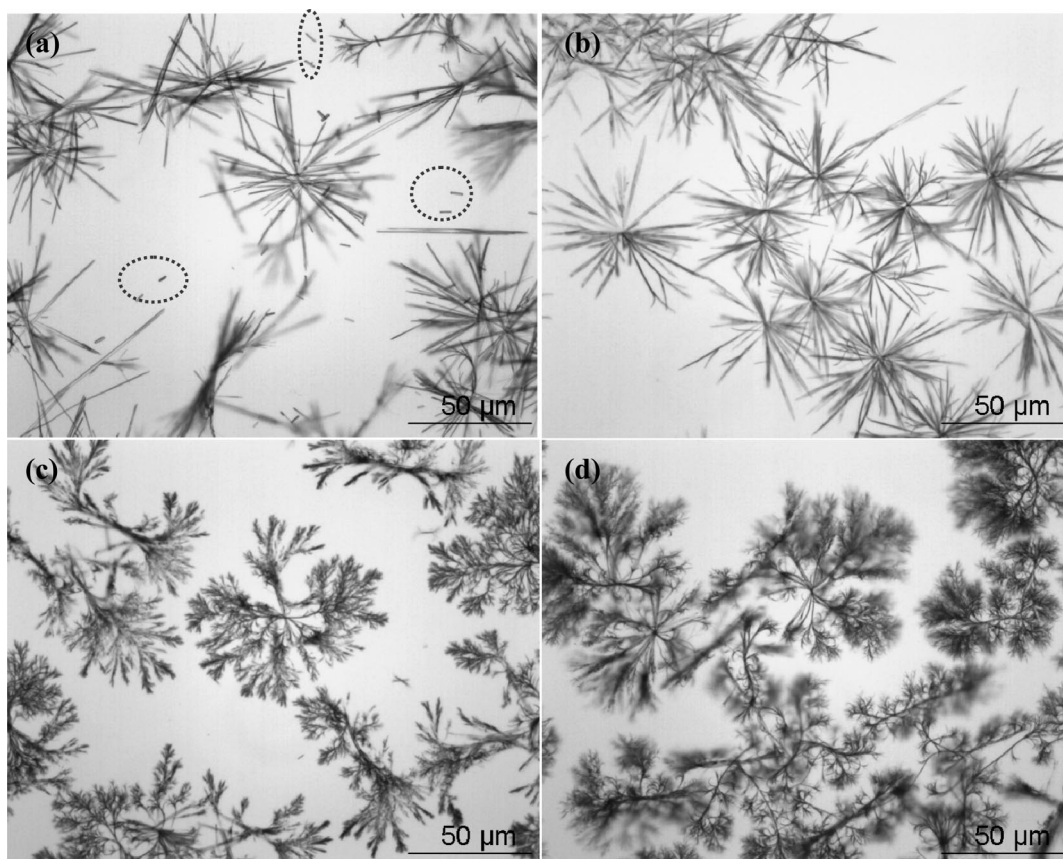


**Figure 4.** NF monohydrate recrystallized from solvents: (a) without any polymer; and from solvent containing (b) PEG; (c) EHEC; and (d) HPMC. Examples of plate-like crystals are circled.

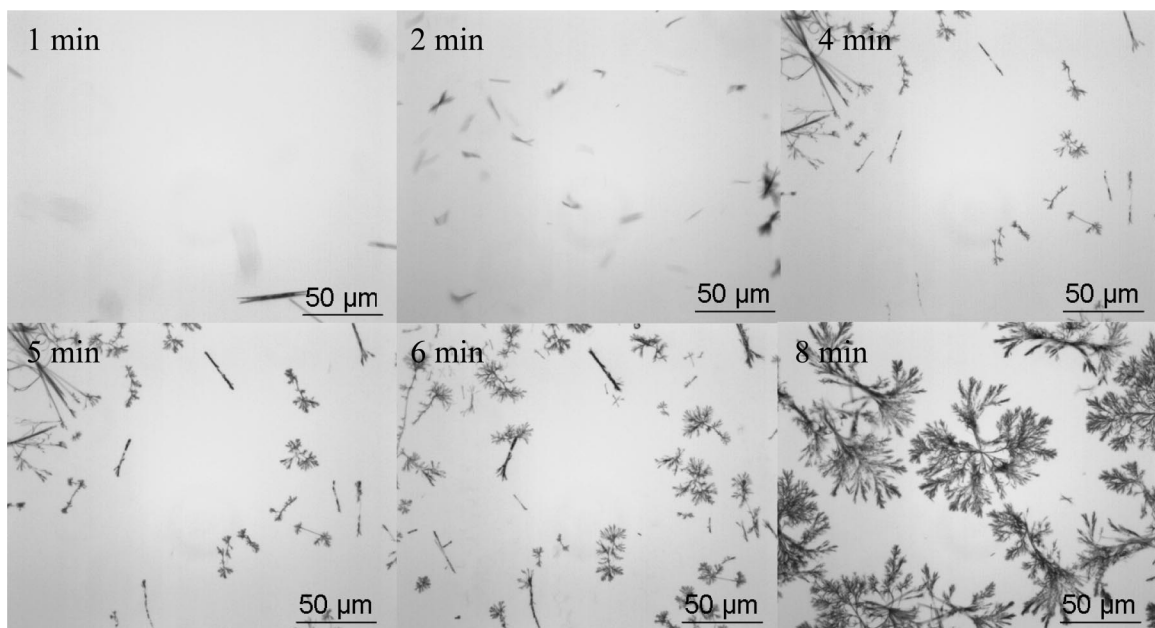


**Figure 5.** Growth of dendrite-like crystals in the presence of EHEC observed under light microscopy. The time point at which each picture was taken is noted in the figure.

crystallized in the presence of polymers (Figure 8e–g), which all exhibited the O–H bonding at the same position and of the same shape as that of pure monohydrate II. Marked differences were noticed for the C=O bands,

though. The one crystallized from solution containing PEG had a slightly increased peak intensity for hydrogen bonded C=O (Figure 8e). In the presence of EHEC, the intensity of this bonded C=O was further increased

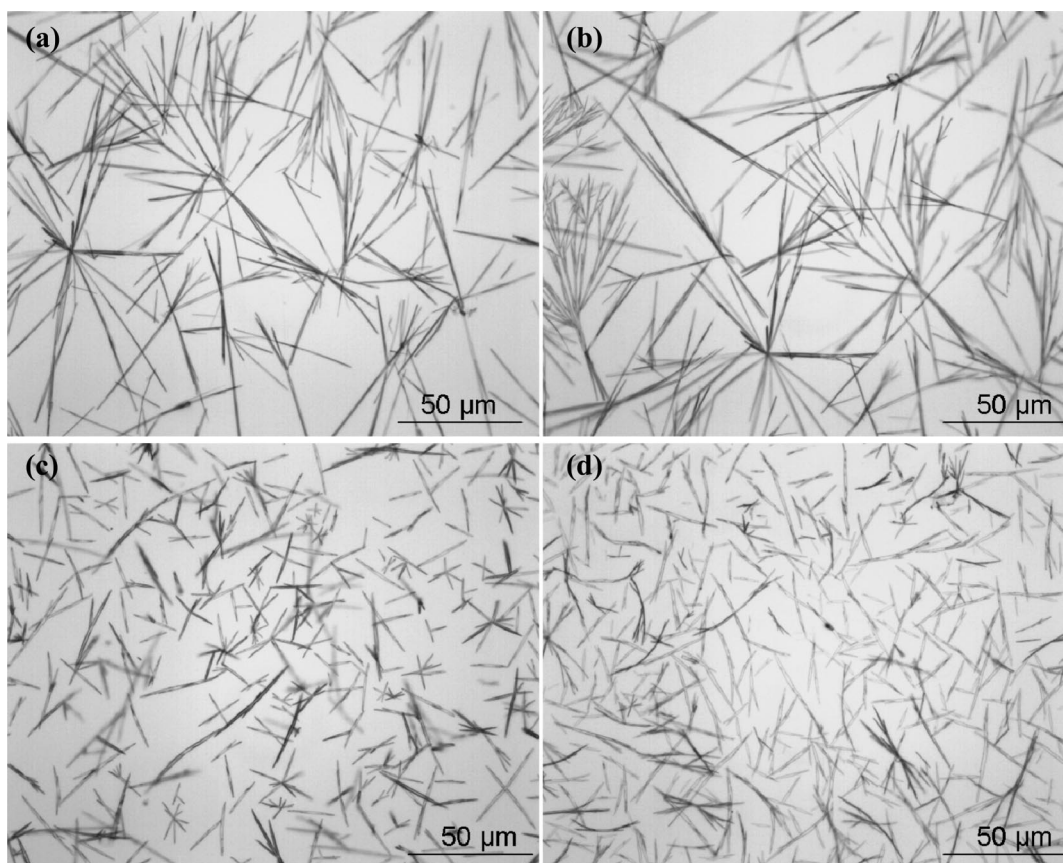


**Figure 6.** CBZ dihydrate recrystallized from solvent: (a) without any polymer; and from solvent containing (b) PEG; (c) EHEC; and (d) HPMC.

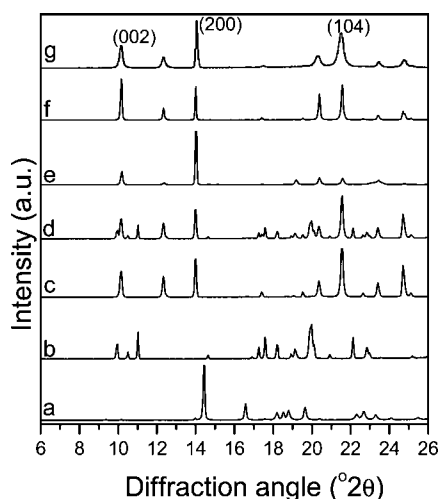


**Figure 7.** XRPD pattern of (a) NF  $\beta$ -polymorph; (b) NF monohydrate I; (c) NF monohydrate II; (d) recrystallized NF from solvent containing no polymer; and from solvent containing (e) PEG; (f) EHEC; and (g) HPMC.

(Figure 8f). Moreover, a dramatically increased peak intensity of this band was obtained for the monohydrate crystallized in the presence of HPMC (Figure 8g), while the free C=O band almost disappeared.

The IR results of all crystallized CBZ products confirm again that none of the additives had any influence on the crystallization outcome of CBZ. Also, no H-bonding was

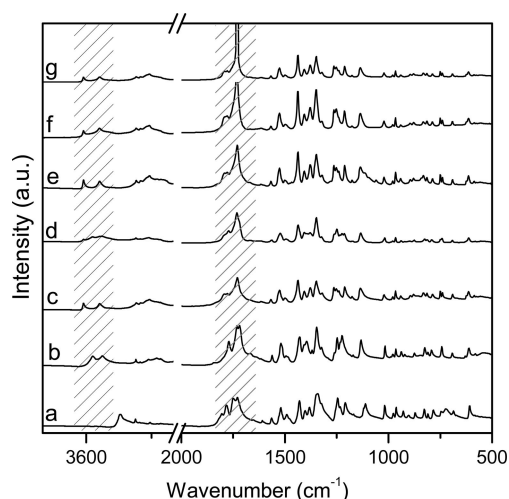


**Figure 8.** FT-IR spectra of (a) NF  $\beta$ -polymorph; (b) NF monohydrate I; (c) NF monohydrate II; (d) crystallized NF from solvent containing no polymer; and from solvent containing (e) PEG; (f) EHEC; and (g) HPMC.

shown to be formed between CBZ and any of the additives (data not shown).

## Discussion

The rheology data revealed that both EHEC and HPMC solutions had a high viscosity and associated network, which is a possible explanation for their modification of dendrite-

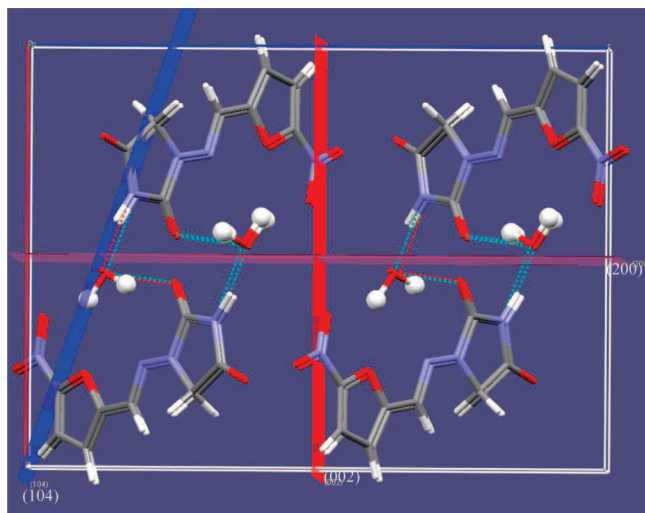


**Figure 9.** Crystal structures of three planes, (002), (200) and (104).

like growth of NF hydrate crystals. However, PEG, which showed only a slight increase in viscosity with no sign of network associations, had no such effect. The dendrite-like crystals exhibited numerous branches, which appeared to be produced via an abundant number of interactions between the drug and the polymer. Also, when comparing EHEC and HPMC, the HPMC system showed more cross-links in the network, and the growth of the NF crystals was observed to involve more condensed dendrite-like crystals.

Even though the polymers used were the same in the systems containing EHEC and HPMC, with the same H-bonding sites and the same network associations, they only had a slight effect on the growth direction of CBZ dihydrate crystals. The diffusion of molecules in a polymer network depends upon the structure and mobility of the matrix, the size of the molecule and specific interactions between the cosolute and the matrix polymer. Baldursdottir et al. have shown that the network structure plays a major role in the diffusion of molecules in the matrices. Evolution of a tighter network inhibits the diffusion of the molecules in the matrix.<sup>19</sup> Therefore, the restriction of movement, which reduces the solute supply to the crystal surface by diffusion, might be the reason for the restricted elongation of CBZ dihydrate needles.

XRPD demonstrated that all crystallized NF from polymer-containing solutions was monohydrate II regardless of their varied morphology. The difference in the intensity of relative peaks could be due to preferential exposure of their associated molecular packing when they are crystallized with different additives. As illustrated in Figure 9 below, plane (104) exposing active carbonyl groups and plane (200) intersecting the H-bonding net in NF monohydrate II could both be expected to be influenced by the presence of additive,

(19) Baldursdóttir, S. G.; Kjoniksen, A.-L.; Nyström, B. The effect of riboflavin-photoinduced degradation of alginate matrices on the diffusion of poly(oxyethylene) probes in the polymer network. *Eur. Polym. J.* **2006**, *42*, 3050–3058.

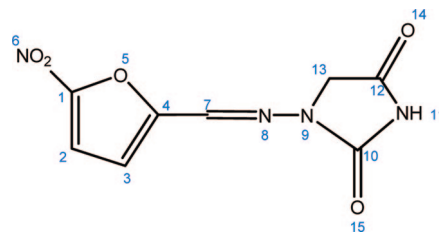


**Figure 10.** Chemical structure of NF anhydrate.

since the existence of H-bonding between crystallized NF monohydrate II (C=O group) and polymers (O–H group) has been verified (described in more detail later). Although no clear active H-bonding sites are related to plane (002), it is certainly involved in the packing of monohydrate II and is thus susceptible to changes in the final crystal properties, for instance in the crystalline form. Moreover, a slight diffraction broadening was noticed in the XRPD diffractogram of the NF recrystallized from the HPMC containing solution. One plausible explanation is that a certain amount of HPMC had been adsorbed to NF crystals during crystallization, so that a diffraction broadening was observed in XRPD.

FT-IR results (Figure 8), which reflect the vibrations of polar groups, further proved the existence and forces of the H-bonds between each polymer and NF monohydrate II. The increased band intensity of bonded C=O (shaded in gray in Figure 8) suggests an increased bonding degree of this carbonyl group in the NF monohydrate, following an order of PEG (only slightly bonded) < EHEC < HPMC. This agrees with the H-bonding ability of the additives as seen from their chemical structures (Figure 1). PEG is the weakest one, because it only has hydrogen bond donor groups at the two ends of the polymer chain and has a relatively weak hydrogen bond acceptor. HPMC and EHEC have both hydrogen bond donor and acceptor groups in their ring structure, and the H-bonding ability is EHEC < HPMC.<sup>20,21</sup> Moreover, as mentioned in the rheology section, the HPMC network had the highest network associations, and this contributes to restraints in the diffusivity of the drug molecule. Both the fact that the HPMC network has the highest H-bonding ability and the highest network associations could be factors contributing to the strongest bonding being between HPMC and dissolved NF molecules. Additionally, EHEC is composed of a cellulose backbone and has ethylene glycol and/or short poly(ethylene glycol) side chains which can sterically hinder H-bonding for the hy-

(20) Tian, F.; Saville, D. J.; Gordon, K. C.; Strachan, C. J.; Zeitler, J. A.; Sandler, N.; Rades, T. The influence of various excipients on the conversion kinetics of carbamazepine polymorphs in aqueous suspension. *J. Pharm. Pharmacol.* **2006**, *59*, 193–201.

(21) Singh, S. K.; Nilsson, S. Thermodynamics of Interaction between Some Cellulose Ethers and SDS by Titration Microcalorimetry: I. EHEC and HPMC. *J. Colloid Interface Sci.* **1999**, *213*, 133–151.

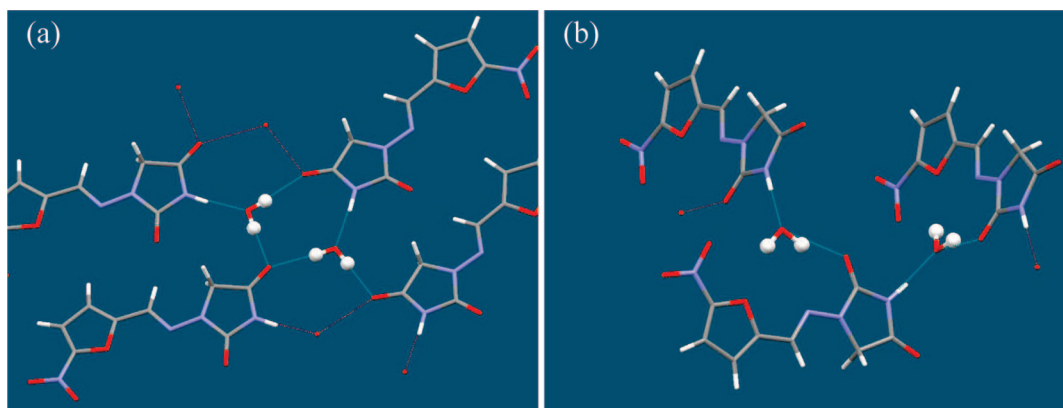


**Figure 11.** Crystal structure of NF hydrate I (a) and II (b) as characterized by hydrogen bonding.

droxyl groups on the backbone.<sup>22</sup> The side chains of HPMC are shorter than those of EHEC, and therefore, the HPMC is not expected to have the same restraints.

Because it is now recognized that hydrogen bonding exists between the drug and the additives, the potential H-bonding sites from the NF molecule were closely scrutinized. The atom N11 (Figure 10) is a relatively strong H-bond donor, which has the highest potential for H-bonding with the oxygen atom from the water molecules and thus forms NF monohydrate. Theoretically, the two oxygen atoms (O14 and O15 in Figure 10) also have certain H-bonding acceptor ability. In other words they might also be H-bonded with the hydrogen atom in water molecules. In order to further probe the exact packing and H-bonding arrangement in NF hydrates, their crystal structures, as characterized by H-bonding, were explored (shown in Figure 11).

NF monohydrate I is formed by connection of the N11 of NF molecule and the O atom (water), where both H atoms of a water molecule were also H-bonded with the O15 (carbonyl group) from two different NF molecules. The connections are indicated by the green dotted line in Figure 11a.

In NF monohydrate II, the monohydrate formation is through the linkage of  $N11 \cdots O-H$  (water), where  $O-H$  (water) is also linked to O15 (second NF monohydrate). Therefore, each water molecule in monohydrate II links two nitrofurantoin monomolecules by hydrogen bonding. However, a series of other hydrogen bonds also exist in NF monohydrate II as suggested by Pienaar et al.<sup>12</sup> The distances  $O$  (water)  $\cdots O$  ( $NO_2$ ),  $O$  (water)  $\cdots O5$ ,  $O$  (water)  $\cdots O14$ , and  $O$  (water)  $\cdots N8$  are all in the range 2.961(4)–3.211(4) Å, indicating weak and possibly bifurcate hydrogen bonds. Intermolecular contact  $C7-H7 \cdots O15$  also showed a geometry meeting the criteria for a hydrogen bond. Therefore, there was a complex hydrogen bonding scheme in NF monohydrate II. This feature sets NF monohydrate apart from most other hydrates (as exemplified by CBZ later).

In contrast to nitrofurantoin, no H-bonding was found between CBZ dihydrate and the polymer additives. The

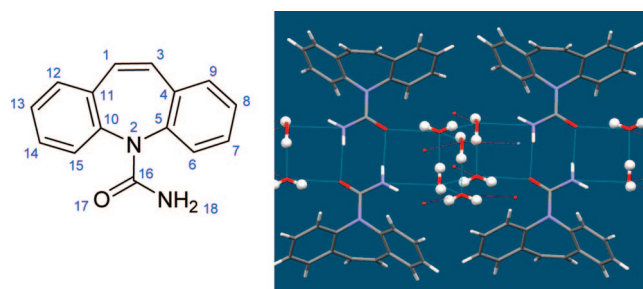


**Figure 12.** Chemical structure of CBZ anhydrate (left); and crystal structure of CBZ dihydrate as characterized by hydrogen bonding (right).

interacting potentials between the CBZ and the polymer additives were thus explored in an attempt to understand the difference in the interaction between these two drugs.

The two hydrogen bonding atoms from CBZ were O17 and N18 (Figure 12, left). When forming a dihydrate, both of these two atoms were H-bonded with two separate water molecules (Figure 12, right). There is no free hydrogen bonding site left in CBZ dihydrate, which contrasts with the case for NF monohydrate II. Therefore, it is highly unlikely that the polymers could H-bond with CBZ dihydrate crystals.

Therefore, the lack of H-bonding sites of CBZ dihydrate, and thus the absence of its H-bonding interaction with the additives, is the main reason for the decreased influence of the additives on crystallization. The shortened needle elongation of CBZ needle crystals by EHEC and HPMC is most likely due to their viscosity and network associations, as explained earlier in the rheology section.

Although there is a possibility that a very small amount of additives, particularly HPMC, has been adsorbed to the NF crystals during crystallization, as suggested for XRPD above, the adsorption degree is expected to be insignificant, since no polymer signal could be detected by IR or Raman spectroscopy. As acknowledged, the desirable additives should be very effective in crystal modification, but have no contamination on API crystals, the degree of polymer adsorption to the drug particles is currently being examined. A number of earlier studies have established that surface adsorption of polymer additives can have positive effects

(22) Kapsabelis, S.; Prestidge, C. A. Adsorption of Ethyl(hydroxyethyl)cellulose onto Silica Particles: The Role of Surface Chemistry and Temperature. *J. Colloid Interface Sci.* **2000**, 228, 297–305.

on drug performance, for instance on dissolution rate.<sup>23,24</sup> It is therefore of interest to evaluate the physicochemical properties of NF monohydrate crystals having dendrite-like morphology.

- 
- (23) Sarkari, M.; Brown, J.; Chen, X.; Swinnea, S.; Williams, R. O.; Johnston, K. P. Enhanced drug dissolution using evaporative precipitation into aqueous solution. *Int. J. Pharm.* **2002**, *243*, 17–31.
- (24) Sinswat, P.; Gao, X.; Yacaman, M. J.; Williams, R. O.; Johnston, K. P. Stabilizer choice for rapid dissolving high potency itraconazole particles formed by evaporative precipitation into aqueous solution. *Int. J. Pharm.* **2005**, *302*, 113–124.

## Conclusions

This study provided an insight into the role of polymer additives on the crystallization of hydrate compounds. The data presented in this study confirmed that additives affect the crystallization of drugs via their H-bonding with the compound and also by increasing viscosity and network associations in the system. The presence of available H-bonding sites on both a compound and a polymer is the first prerequisite for ensuring strong interactions, and thus successful crystal modification.

MP800142Z